Proceedings of the 2006 IEEE
International Conference on Control Applications
Munich, Germany, October 4-6, 2006

Modeling and Control of a Four Wheel Drive Parallel Hybrid Electric Vehicle

Ali Boyalı, Murat Demirci, Tankut Acarman *member IEEE*, Levent Güvenç, *member IEEE*,
Okan Tür, Hamdi Uçarol, Burak Kiray, Evren Özatay

***Abstract*—Modeling and control of a hybrid electric vehicle is presented in this paper. A four wheel drive parallel hybrid electric vehicle is built by assembling an auxiliary electrical machine and battery group. Some preliminary instrumentation such as accelerator pedal, brake, clutch pedal position sensors and gear ratio estimation are realized to split torque demand into the two power sources. The first power source is the internal combustion engine and the second one is the permanent magnet electric motor. A rule-based control strategy is developed by setting transition rules between the two power sources. The control strategy is implemented on a proof-of-concept vehicle and road tested. In order to satisfy smooth transient switching between the two power sources, and in order not to disturb the driver by abrupt or retarded transitions, torque splitting is achieved by taking the power source dynamics and vehicle dynamics in the longitudinal direction into account. The internal combustion engine is not operated at its high emission and low fuel efficient regions. Regenerative braking is implemented to charge the electric motor battery pack during braking.**

Index Terms—Automotive control, hybrid electric vehicle modeling, hybrid electric vehicle control, rule-based control.

I. INTRODUCTION

Increasing levels of health-threatening air pollution, necessitate governments around the globe to take stringent measures to reduce them. In this respect, pollutant gases emitted by on road motor vehicles is a major concern since their contribution to air pollution is considerably high. The new regulations on motor vehicle emissions force car manufacturers to develop new technologies for reducing undesired vehicle emissions. Car manufacturers have, thus, been searching for ways of improving engine efficiency while staying within the limits stipulated by the legislated standards. Despite outstanding developments, internal combustion engine (ICE) technology is still far away from meeting the emission standard requirements proposed for the near future.

Internal combustion engines are designed for operating at high loads as efficiently as they can. In urban driving, the ICE is usually operated at undesirable operating points with high fuel consumption and high emissions [2]. At cruise speeds, on the other hand, the ICE may be operated at lower torque values. At high loads, even an efficiency of 40% is not acceptable with regard to today's technologies. The remedy is to find new renewable energy sources.

New energy sources such as fuel cell, pure electric energy and hydrogen are emerging technologies but their practical use is currently unfeasible due to the high costs involved. Car manufacturers tend to find acceptable intermediate solutions such as Hybrid Electric Vehicles (HEV) in which an electric motor is used along with the conventional internal combustion engine.

The main challenge is to control power sources efficiently. There are ongoing researches on HEV control algorithms. HEV control algorithms, proposed in the literature, may be classified into three categories depending on the control methodology used as rule based control, global optimal control and local optimization approaches [4]. The main problem in HEV control applications is to find the adequate torque split combination of ICE and electric motor (EM) required to minimize fuel usage and emissions while the vehicle is requesting power with different speed characteristics.

The calculations for the adequate combination mentioned above should take into account the losses in the transmission and the non-ideal characteristics of the batteries. As an extreme example, note that the optimum choice for reducing fuel consumption alone is to operate the vehicle with pure electric energy. This is not possible as current battery technology can not store enough energy for reasonable travel mileage between charging stops even in urban driving.

In HEV control, the aim is to find an optimum path for the conversion of energies. There are several studies in this area. In rule based control, simple rules are used in order to split the power between the two sources [5]. Fuzzy logic control is one approach under this category. In fuzzy logic control, the rules are scaled in membership functions. In a simple rule based algorithm, decisions are made between only two choices. In contrast, choices in between the boundary decisions are possible in fuzzy logic control [6].

The second control approach is global optimization. In this approach, dynamic programming is used to find the

A. Boyalı, M. Demirci and L. Güvenç are with the İstanbul Technical University, Mechanical Engineering Department, İstanbul/Turkey, (e-mail: {ali.boyali, murat.demirci, guvencl}@itu.edu.tr, phone: +90 212 251 6563).

T. Acarman is with Galatasaray University, Faculty of Engineering and Technology (e-mail: tacarman@gsu.edu.tr).

O. Tür and H. Uçarol are with the Scientific and Technological Research Council of Turkey, Marmara Research Center, Energy Institute, (e-mail: {okan.tur, hamdi.ucarol}@mam.gov.tr).

B. Kiray and E. Özatay are with Ford-Otosan, Product Development, R&D Department, Kocaeli/Turkey, (e-mail: {bkiray, eozatay}@ford.com.tr).

optimum operating path. To find the optimal operating points, it is necessary to know the whole speed profile in advance. This is not possible in real driving. The actual speed profile depends on the driver and traffic conditions. To cope with this kind of uncertainty, the optimization problem should be reduced to a local optimization problem. There are two approaches to local optimization. The first one is point wise optimization and the second one is interval optimization.

In point-wise optimization techniques, the equivalent energy consumption is computed at several operating points and minimizing control variables are computed offline [7] - [10]. An example of interval optimization is model predictive control. In model predictive control, the actual driving cycle is divided into small intervals and the speed profile is estimated using past vehicle speed [11]. A simple rule based algorithm for power distribution management is concentrated upon here.

This paper is on modeling and control of a four wheel drive parallel hybrid electric vehicle. The organization of the paper is as follows. Modeling of the hybrid electric vehicle is presented in section II. The rule based torque-split control strategy design is considered in section III. The proof-of-concept experimental vehicle used for controller implementation is described in section IV. Simulation and experimental results are given in section V. The paper ends with some conclusions and discussions.

II. MODELING 4WD HYBRID ELECTRIC VEHICLES

The Ford Transit commercial van was selected as the proof-of-concept experimental vehicle. It has enough payload and space to add an electric motor, the required battery pack, and the necessary electronic and control modules. Both front and rear wheel drive versions of the Ford Transit are available. Adding a rear wheel drive unit powered by an electric motor to a front wheel drive Ford Transit, therefore, resulted in a parallel, four wheel drive (4WD) hybrid electric vehicle. This approach simplified mechanical construction of the experimental vehicle.

The forward flow technique of modeling the hybrid electric vehicle dynamics is used here. The engine model is fed the throttle position and the engine speed, and the torque required to drive the vehicle is computed as illustrated in Fig. 1.

The forward computation method is more convenient for analyzing different velocity profiles and reflects the realistic nature of driver intention. There are three commands generated by the driver. These are the accelerator, brake and clutch pedal commands. The accelerator and brake pedal commands are in the range of 0-100% of their maximum possible openings while the clutch pedal command takes the digital values of "0" for its unpressed and "1" for its pressed position.

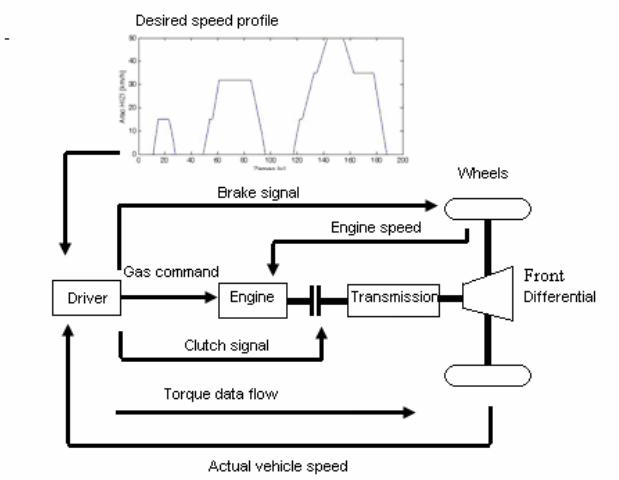

Fig. 1. Forward data flow computation technique and typical urban driving speed profile

A. Tire Model and Longitudinal Dynamics

In this study, the Pacejka 2002 tire model is used (see ref. [1]). The Pacejka 2002 tire model longitudinal tire force $F_x(s)$ as a function of longitudinal slip ratio is given by

$$F_x = D\cos[C\text{atan}(B - \text{atan}(B))] \tag{1}$$

Equations similar to (1) above exist in the Pacejka 2002 tire model for the other tire force components and tire moments. The parameters B, C, D on the right hand side of equation (1) are empirically determined coefficients which depend on several other empirically determined coefficients and the longitudinal wheel slip s. The coefficient values are different for different tires. The inputs and outputs of the general tire model are shown in Fig. 2.

Here, F_x and F_y are the longitudinal and lateral tire forces. M_x, M_y and M_z are the over-turning, rolling resistance and aligning moments, respectively. Although a fairly detailed tire model was prepared, only its longitudinal force computation capability is used at the simulations.

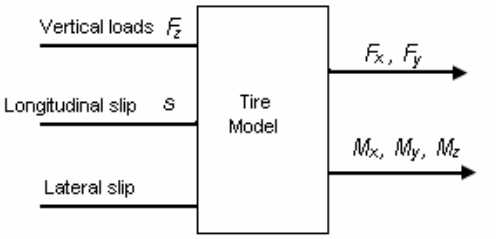

Fig.2. Tire model input and outputs

Longitudinal tire force depends on the longitudinal wheel slip ratio given by

$$s = \begin{cases} \dfrac{R\omega - V}{V}, & R\omega < V \quad (braking) \\ \dfrac{R\omega - V}{R\omega}, & R\omega > V \quad (driving) \end{cases} \tag{2}$$

Definitions of the variables are given in the nomenclature section. Calculation of slip ratio using (2) above necessitates the computation of the tire angular velocity. Based on the free body diagrams in Fig. 3,

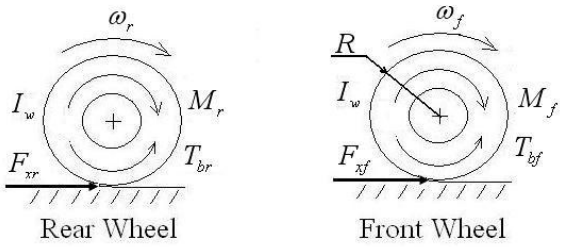

Fig. 3. Torques acting on front and rear tires

the moment balances give,

$$M_r - T_{br} - F_{xr}R = I_w\dot{\omega}_r \quad (3)$$

$$M_f - T_{bf} - F_{xf}R = I_w\dot{\omega}_f \quad (4)$$

The external forces acting on the vehicle in the longitudinal direction are the longitudinal tire, aerodynamic, rolling resistance, gradient resistance and acceleration resistance forces. These forces are displayed graphically in Fig. 4.

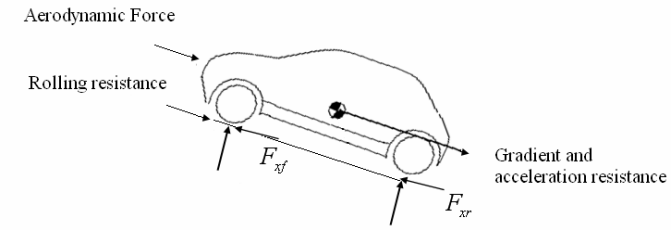

Fig. 4. Longitudinal forces acting on the vehicle

Aerodynamic force is calculated as

$$F_a = \frac{1}{2}A\rho C_D V_{rel}^2 \quad (5)$$

Gradient force is computed using

$$F_g = W\sin(\theta) \quad (6)$$

Rolling resistance is formulated using the SAE J2452 standard as

$$F_r = P^{\alpha}W_t^{\beta}(a + bV + cV^2) \quad (7)$$

The net force acting in the longitudinal direction on the vehicle is calculated using

$$F_{net} = \lambda m a_x = F_{xf} + F_{xr} - F_a - F_g - F_r \quad (8)$$

B. Transmission and Engine

The transmission and other driveline components, shown in Fig. 5 are modeled as rigid bodies given by

$$M_{ice}i_g\eta_g = M_t, \quad (9)$$

$$M_t i_{fd}\eta_{fd} = M_f, \quad (10)$$

$$M_{em}i_{rd}\eta_{rd} = M_r, \quad (11)$$

for the front and rear drives. The proposed hybrid concept is a 4WD hybrid electric vehicle, where the front axle is excited by an internal combustion engine, and the rear axle is excited by an electric motor as illustrated in Fig. 5.

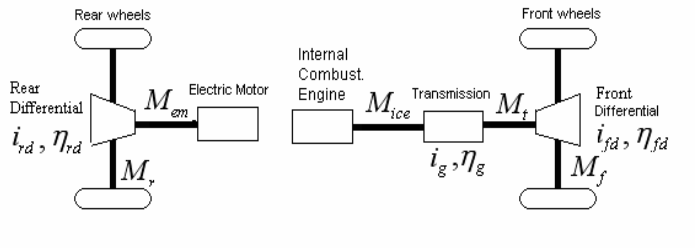

Fig. 5. Driveline components

The engine is modeled using a static engine map from throttle command and engine speed to engine torque. A typical two-dimensional static engine map with extra curves displaying fuel consumption rate is displayed in Fig. 6.

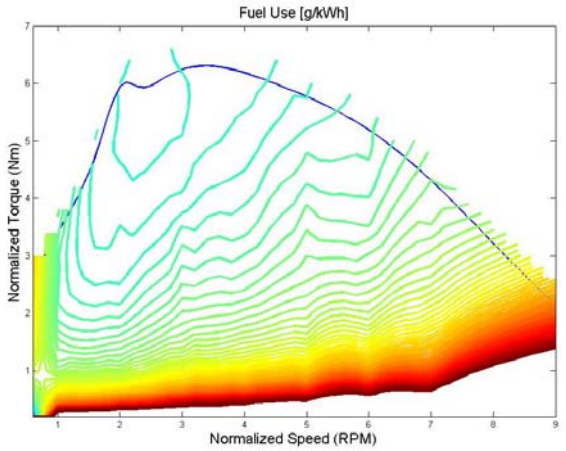

Fig. 6. Engine Fuel Consumption Map

C. Battery and Electric Motor Model

A simple equivalent circuit is used to model the battery group. The open circuit voltage V_{oc} and internal resistance $R_{int,}$ depending on state of charge and current flow direction, are used in

$$V_{bat} = V_{oc} + I_{bat} R_{\text{int}} \tag{12}$$

to obtain the battery output voltage V_{bat}. Electric vehicle applications require high steady power to torque ratio, typically in the range of 3 to 5 for better performance at lower power consumption [3]. For simplification of the overall electric traction system modeling, a permanent magnet direct current motor model is used.

Conventional permanent magnet stator DC machine model equations can be modified as below to simulate the constant power region of a field orientation controlled AC machine

$$V_a = E_a + R_i I_a + L_i \frac{dI_a}{dt}, \tag{13}$$

$$E_a = k_e(w_r) w_r , \tag{14}$$

$$T_e = k_t(w_r) I_a , \tag{15}$$

as illustrated in Fig. 7.

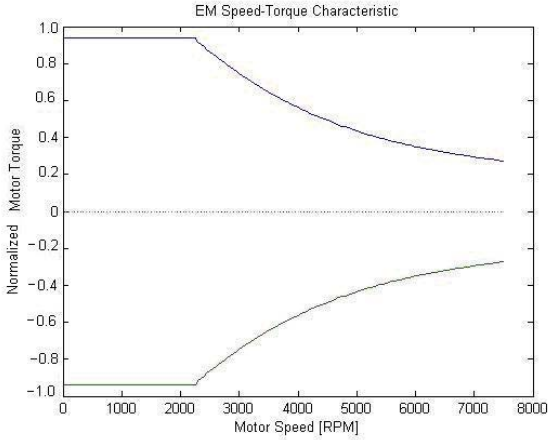

Fig. 7. EM Torque – Rotor Speed characteristics

III. CONTROL STRATEGY

A. *Rule Based Algorithm*

The rule based algorithm used here switches between five main states. These states are:

- Standstill vehicle position (Standstill mode)
- Pure EM excitation (EM mode)
- Pure ICE excitation (ICE mode)
- Charging or EM assist (Hybrid mode)
- Braking mode

These states are the main states for a parallel hybrid electric vehicle configuration. The transitions are defined by switching rules in rule based control. The states and switching rules are illustrated in the Stateflow chart in Fig.8.

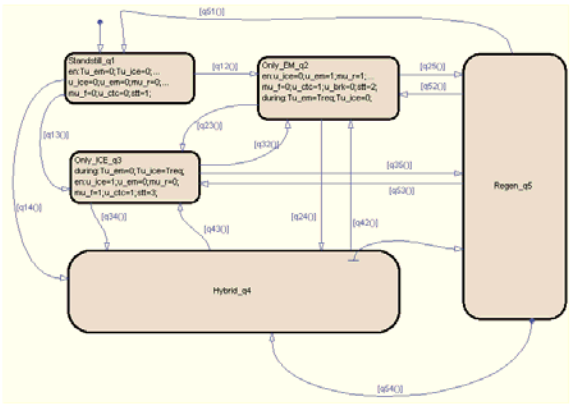

Fig. 8. State flow diagram of the proposed rule based HEV control algorithm

In optimization based algorithms, the objective of transition between modes of operation is to maintain the operating point at the optimum value.

B. *Vehicle States*

Vehicle states are defined to be the standstill, EM, ICE, hybrid (charge and assist) and braking mode.

1) *Standstill Mode*

In standstill position, the vehicle velocity is less than a certain predetermined value like 5 km/hr. In this state, there is no command generated by the driver. If the driver presses the accelerator pedal, the Stateflow chart may enter into three other states. These are the EM, ICE or hybrid (EM assist part) modes.

2) *EM Mode*

If the battery state of charge (SOC) is sufficiently high, and the required torque does not exceed the maximum EM torque output, the default state is always chosen as the EM state, i.e. using only the EM.

Three transitions are allowed from the EM mode to other states. The first two transitions are dependent on the power demand at the wheels. When the required power exceeds the power threshold, that is 6 kW, the state is shifted to the ICE mode. During kick-down, (accelerator pedal position exceeds 70% of its travel range), the hybrid mode in which the EM assisting the ICE becomes active. The vehicle becomes a four wheel drive (4WD) hybrid electric vehicle in this mode. The braking mode is switched on when the brake pedal is pressed. Otherwise, the EM mode is maintained.

Accelerator pedal displacement is evaluated as an indication of power demand input by the driver. Once the accelerator pedal displacement and ICE motor speed are sensed by the electronic control unit (ECU), the corresponding torque request is computed using the pedal map shown in Fig.9.

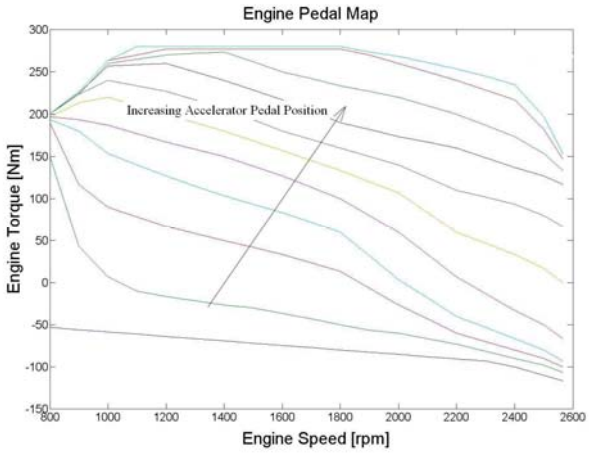

Fig. 9. Engine pedal map versus engine speed and engine torque characteristics

Two kinds of transition are possible. If an accurate engine map, i.e., torque output versus ICE speed, is available, an inverse map can be used to distribute required torque between the EM and the ICE. Another easier approach is to calibrate the accelerator pedal position in such a way that the EM generates the same amount of torque as the ICE for the same pedal position. For smooth transitions between the states, time dependent smooth transition functions such as rate limiter, saturation functions or sigmoid functions are used.

3) ICE Mode

If the energy stored in the batteries is low and if the requested power does not exceed the ICE's power output at the measured speed, only the ICE powers the vehicle. If the driver fully presses the accelerator pedal, i.e. kick-down, the hybrid mode is switched on and the EM assists the ICE. If the driver presses the brake pedal, the braking mode is activated. Otherwise, the ICE mode is maintained.

4) Charge and Assist Mode

The EM is operated as a generator to recharge the batteries and maintain their state of charge. Efficiencies of the battery, the EM and the ICE are crucial while generating electrical energy. In the actual experimental and simulation studies, a constant charge torque level was used. In the charging mode, the ICE was rendered capable of meeting the electrical energy generation and traction force requirements.

If the accelerator pedal position exceeds 70% of its full range, the power assist mode is entered and the EM starts assisting the ICE to provide more power. For a smooth transition, the additional EM assist moment is increased parabolically to its maximum value at 100% accelerator pedal position. At full accelerator pedal opening, both the ICE and the EM generate their maximum power.

5) Braking Mode

If the brake pedal is pressed, the braking mode becomes active. Transition into one of two sub-states is possible. If the battery state of charge is less than the allowed level, regenerative braking is activated in the allocated brake pedal force region. If the battery state of charge is at the allowed maximum limit, regenerative braking is disabled. Regenerative braking is designed carefully to transform the maximum transformable kinetic energy into electrical energy during braking and avoiding wheel lock-up.

IV. PROOF-OF-CONCEPT VEHICLE IMPLEMENTATION

The proof-of-concept experimental vehicle was converted from a front wheel drive vehicle with manual transmission. The presence of the manual transmission and the clutch pedal create a major obstacle in conversion into a hybrid electric vehicle. As the vehicle is usually driven by the rear drive EM at low speeds and by the ICE at higher speeds, the best solution is to make sure that the driver can drive the vehicle as if it is the original vehicle running with the ICE alone. In this manner, he will use the clutch and gear stick as he is used to in a manual transmission vehicle even though they are not needed for pure EM operation at low speeds. During operation of the EM, the ICE is on.

In the experimental vehicle, the accelerator pedal to ICE electronic control unit cables are tapped into. The accelerator pedal position potentiometers are read by the additional HEV electronic control unit, a dSpace microautobox and rapidpro combination, and processed and sent to the ICE electronic control unit. It is possible to interpret the driver torque demand based on the ICE map of the original vehicle, split that demand between the ICE and EM, and send the necessary commands to the ICE electronic control unit and the EM driver with this implementation.

The clutch pedal is pressed by the driver while shifting gear. The ICE torque is changed in an open loop fashion by manipulating the accelerator pedal opening signals sent to the ICE electronic control unit. In order to distribute the required torque between the EM and the ICE, the torque requested by the driver from the ICE at the tires is calculated using the engine pedal map and the overall transmission ratio including the differential. The manual gear estimation algorithm used is based on dividing the vehicle speed by the engine speed. Gear ratio position is estimated by using the upper and lower variations of this division. The gear position estimation is carried out using a Stateflow diagram in Simulink.

V. SIMULATION AND EXPERIMENTAL RESULTS

A. Simulations

Simulink was used for simulating the parallel 4WD hybrid electric vehicle dynamic model presented in section II. The

European Urban Drive Cycle (EUDC) was used as the vehicle velocity profile to be followed during the simulations. A PID driver model was developed and used for tracking the drive cycle velocity profile. If the EM and ICE operate below and above 6 kW of power request, respectively, the fuel savings achieved reaches up to 18%. The drive cycle velocity profile and the time responses of the torques delivered at the wheels are shown in Fig. 10. During the deceleration periods of the EUDC, the ICE starts braking due to its internal resistance at low engine speeds and zero accelerator pedal position. This is the reason for the negative ICE moments in Fig. 10.

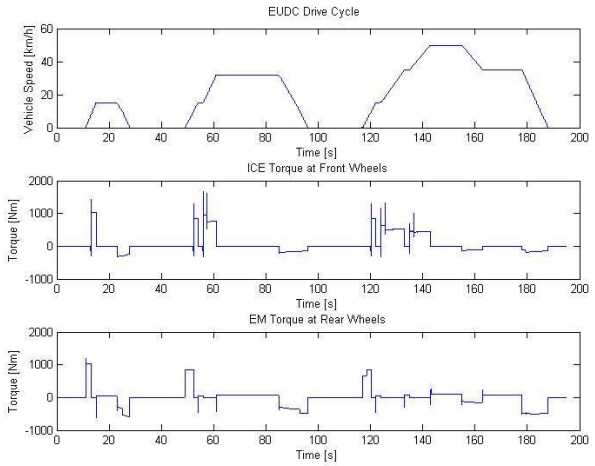

Fig. 10. EM and ICE torques during EUDC at wheels

The operating points traversed during the simulation of the EUDC are shown on the ICE map in Fig. 11. Grid like appereance is the characteristics of drive cycle used.

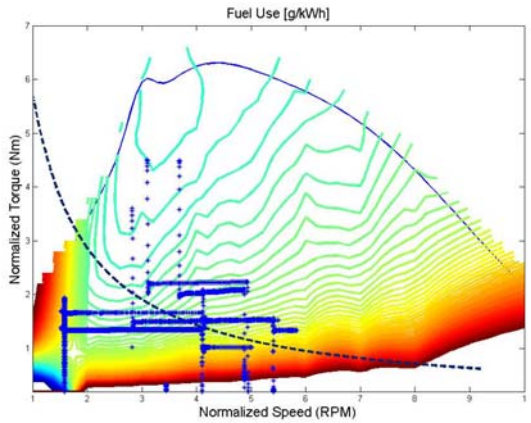

Fig. 11. ICE operating points in EUDC

B. ECU Setup and Experiments

A dSpace MicroAutoBox (MABX) complemented with a RapidPro system was used as the main electronic control unit to run the hybrid electric vehicle control algorithm. The MABX and Rapidpro system installed in the Ford Transit van is shown in Fig. 12.

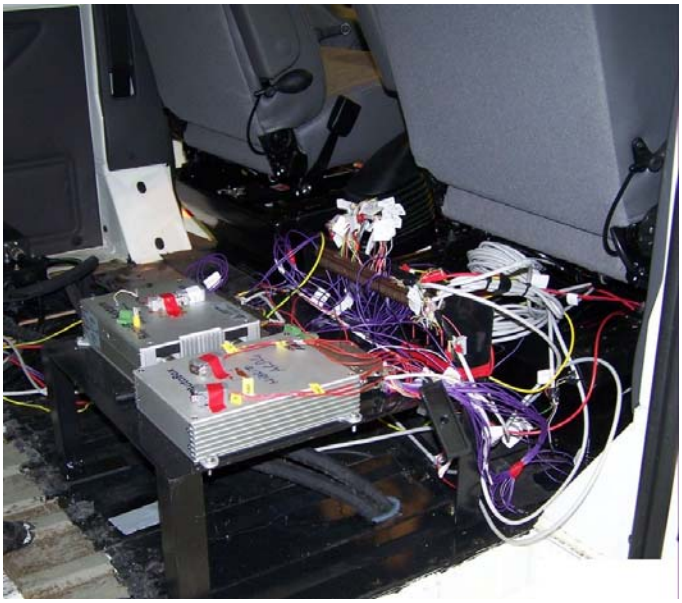

Fig. 12. HEV controller hardware connections in the experimental vehicle

All signals required by the HEV controller were gathered via the MABX and the RapidPro signal conditioning units. The general signal connection diagram is shown in Fig. 13.

The HEV control strategy is modeled in Matlab/Simulink. Automatic code generation and downloading into MABX is handled by the Matlab Real Time Workshop and dSpace Real Time Interface tools as illustrated in Fig. 14.

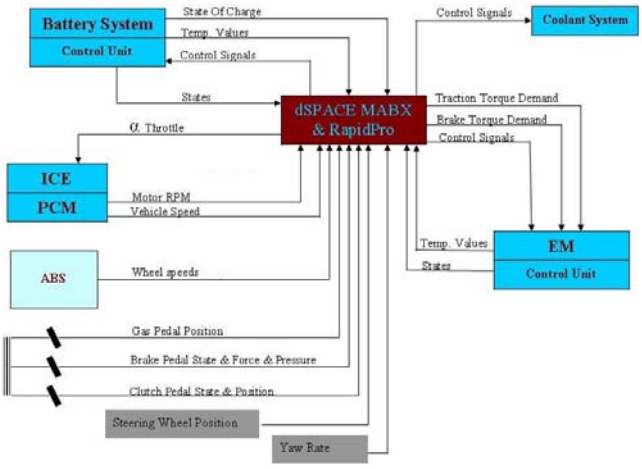

Fig. 13. General signal connection diagram

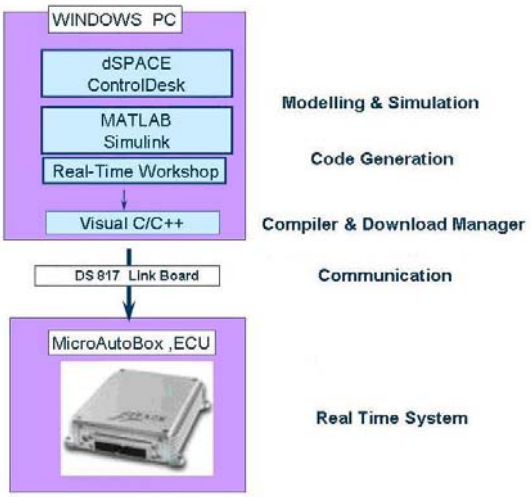

Fig. 14. Rapid HEV control algorithm prototyping process diagram

As seen in Fig. 15, the EM driver enables the conversion of DC voltage to AC voltage. The electric power is supplied by a battery pack which is connected to the motor driver through a circuit breaker as a safety switch.

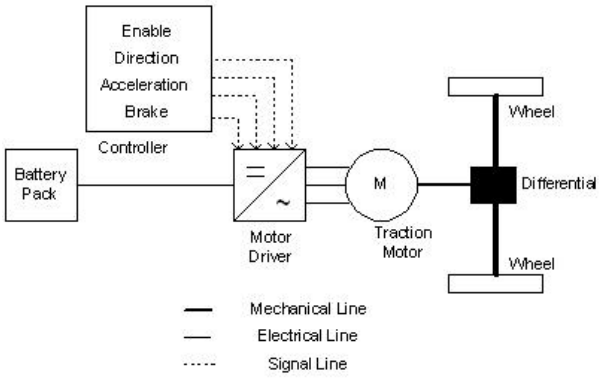

Fig. 15. EM electrical and mechanical connections

The available EM driver control signals (enable, direction, acceleration, brake) allow smooth operation of the EM via its driver. The HEV control unit sends the commands to the controller as acceleration or brake requests. The EM driver applies these requests according to the motor operating region map or generator operating region map.

The HEV controller was fine tuned in road tests to improve drivability. The road tests were successful in terms of drivability and driving feel in the presence of the manual clutch and the manual transmission. Typical road test results are shown in Fig.s 16 and 17.

The estimated gear position, the accelerator pedal command sent to the ICE controller and some of the HEV control strategy modes are displayed in Fig. 16. Most of the modes of the HEV control strategy are entered during the test of Fig. 17. The battery state of charge is maintained in the beginning of the test in Fig. 17 due to regenerative braking. The vehicle operates in the EM mode for a certain time period thereafter. The battery state of charge decreases in the corresponding period. Since the battery state of charge does not drop below its critical lower limit, the charging mode is not entered in Fig. 17 and the state of charge decreases after the end of the regenerative braking mode.

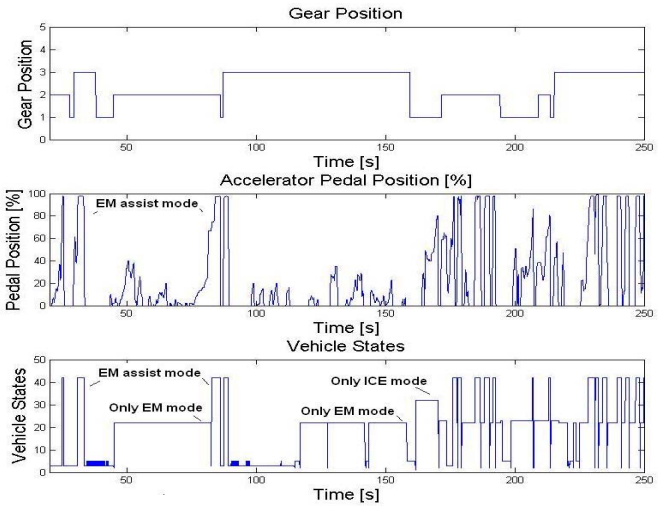

Fig. 16. Experimental results

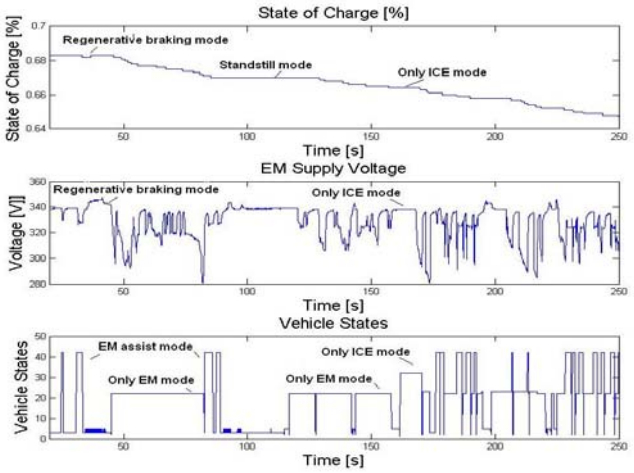

Fig. 17. Experimental result illustrating regenerative braking

VI. CONCLUSIONS

Results on modeling and rule based control of a parallel 4WD hybrid electric vehicle were presented in this paper. The Ford Transit commercial van with its front drive internal combustion engine was equipped with an HEV control system and several sensors. An auxiliary electric motor, capable of providing mechanical energy to power the rear drive and generating electrical energy to recharge the batteries, was assembled into the test vehicle along with a battery pack. A rule based control algorithm was developed to prevent operating the ICE at its poor performance regions. Simulation and experiments were used to

demonstrate the successful results that were achieved. A large number of drivers were asked to drive the proof-of-concept experimental vehicle. Fine tuning for smooth mode transitions based on driver feedback resulted in a vehicle with highly satisfactory drivability and very good driving feel.

Future work will concentrate on optimization methods for HEV control strategy transitions and improvement of handling characteristics of the 4WD vehicle.

ACKNOWLEDGMENTS

The authors thank Ford Otosan R&D Department. The first four authors acknowledge support of the European Union Framework Programme 6 through project INCO-16426.

REFERENCES

[1] Adams Tire User Guide v12.

[2] S. Plotkin, D. Santini, A. Vyas, J. Anderson, M. Wang, J. He, and D. Bharathan, "Hybrid Electric Vehicle Technology Assessment: Methodology, Analytical Issues, and Interim Results," Center for Transportation Research, Energy Systems Division, Argonne National Laboratory, October 2001.

[3] M. Ehsani, "Modern Electric, Hybrid Electric, and Fuel Cell Vehicles: Fundamentals, Theory, and Design," ISBN: 0849331544, CRC Press, December 20, 2004, pp. 102-108.

[4] C. C. Lin, H. Peng, J.W. Grizzle, and J.M. Kang, "Power Management Strategy for a Parallel Hybrid Electric Truck," IEEE Transaction on Control Systems Technology, Vol. 11, No. 6, November 2003.

[5] C. C. Lin, J.M. Kang, J.W. Grizzle, and H. Peng, "Energy Management Strategy for a Parallel Hybrid Electric Truck," Proceedings of the American Control Conference, Arlington, VA, June 25-27, 2001.

[6] N. J. Schouten, M.A. Salman, and N.A. Kheir, "Fuzzy Logic Control for Parallel Hybrid Vehicles," IEEE Transactions on Control Systems Technology, Vol. 10, No. 3, May 2002.

[7] A. Sciarretta, M. Back, and L. Guzzella, "Optimal Control of Parallel Hybrid Electric Vehicles," IEEE Transactions on Control Systems Technology, Vol. 12, No. 3, May 2004.

[8] G. Paganelli, S. Delprat, T.M. Guerra, J. Rimaux, J.J. Santin, "Equivalent Consumption Minimization Strategy for Parallel Hybrid Powertrains," Proceedings of Vehicular Transportation Systems Conference, Atlantic City, NJ, USA, 28-31 October 2001.

[9] V. H. Johnson, K.B. Wipke, and D.J. Rausen, "HEV Control Strategy for Real-Time Optimization of Fuel Economy and Emissions," SAE 2000-01-1543.

[10] G. Paganelli, G. Ercole, A. Brahma, Y. Guezennec, G. Rizzoni, "General supervisory control policy for the energy optimization of charge-sustaining hybrid electric vehicles", JSAE Review 22 (2001) 511–518

[11] S. Jeon, K.B. Kim, S.T. Jo, and J.M. Lee, "Driving Simulation of a Parallel Hybrid Electric Vehicle Using Receding Horizon Control," ISIE, Pusan, Korea, 2001.

TABLE I
LIST OF VARIABLES AND THE PARAMETERS DENOTED

Symbol	Quantity	Unit
F_a	Aerodynamic force	N
A	Front vehicle area	m^2
ρ	Air density	kg/m^3
C_D	Aerodynamic drag coefficient	--
V_{rel}	Relative air velocity	m/s
F_g	Gradient resistance	N
W	Vehicle weight	N
θ	Gradient due to road elevation	rad
P	Tire inflation pressure	kPa
W_t	Normal load on tire	N
a, b, c, α, β	Experimentally determined coefficients	--
V	Vehicle speed	km/h
M_r	Traction moment at rear wheels	Nm
M_f	Traction moment at front wheels	Nm
M_{ice}	Engine generated moment	Nm
M_{em}	EM generated moment	Nm
M_t	Moment at transmission output	Nm
T_{br}	Braking torque at rear wheels	Nm
T_{bf}	Braking torque at rear wheels	Nm
ω_r	Rear wheel angular velocity	rad/s
ω_f	Front wheel angular velocity	rad/s
I_w	Tire inertia	kgm^2
i_g	Transmission gear ratio	--
i_{fd}	Front differential ratio	--
i_{rd}	Rear differential ratio	--
η_g	Transmission efficiency	--
η_{rd}	Rear differential efficiency	--
η_{fd}	Front differential efficiency	--
$F_{xf(r)}$	Traction force at front (rear)wheels	N
λ	Equivalent mass factor	--
V_a	Supply voltage	V
E_a	Back EMF voltage	V
R_i	Winding resistance	Ohm
L_i	Winding inductance	H
k_e	Back EMF constant (rotor flux)	V/ rad/s
k_t	Torque constant	Nm/Amp
w_r	Rotor speed	rad/s
I_a	Motor armature current	A